J. Chem. Eng. Data **1999,** *44,* 613−620

Vapor−Liquid Equilibria for Dendritic-Polymer Solutions

John G. Lieu,[†] Mingjun Liu,[‡] Jean M. J. Frechet,[‡] and John M. Prausnitz*,[†,§]

Chemical Engineering Department, University of California, Berkeley, Department of Chemistry,
University of California, Berkeley, and Chemical Sciences Division, Lawrence Berkeley National Laboratory,
Berkeley, California 94720

Vapor−liquid equilibria for dendritic-polymer solutions were obtained using a classic gravimetric-sorption method; the amount of solvent absorbed by the dendrimer was measured as a function of solvent vapor pressure. Three series of dendrimers, each with the same tertiary amine core structure, but different surface groups, were investigated in a variety of organic solvents in the range 50−75 °C. The dendrimer surface groups were dodecylamines, octadecyl amides, and polyisobutylene. Solvent absorption depends strongly on dendrimer composition and generation number.

Introduction

Dendrimers are macromolecules characterized by highly branched, well-defined structures. They consist of a central core with multiple "arms" radiating outward to form increasingly packed "shells" or "generations." Each arm divides at the same branch point, giving compact three-dimensional patterns.

Precise control of structure, molecular weight, flexibility, and surface chemistry creates a variety of novel applications for dendrimers. In medicine and biotechnology, dendrimers show promise as gene vectors, drug-delivery vehicles, and magnetic-resonance imaging agents. For example, Kukowska-Latallo et al. (1996) demonstrated that dendrimers effectively bind and transfer DNA into a variety of mammalian cells. Jansen et al. (1994) showed that dendrimers can be synthesized to encapsulate guest molecules in a "dendritic box" and that shape-selective liberation of trapped molecules was then possible (Jansen et al., 1995). Dendrimers as magnetic-resonance imaging contrast agents for tumor targeting have been developed (Wiener et al., 1997); they are currently under study for use in mammography (Daldrup et al., 1997). Other biotechnological applications of dendrimers include coupling antibodies to dendrimers for high-performance immunoassays (Singh et al., 1994), oligonucleotide dendrimers for use as polylabeled DNA probes (Shchepinov et al., 1997), and dendrimers as buffer additives in capillary electrophoresis for separation of aromatic amino acids (Gao et al., 1998).

Because dendrimer structure can be accurately controlled, it is possible to construct a single macromolecule with two different moieties, for example dendrimers with an interior hydrophobic core surrounded by a hydrophilic surface layer. Similar to detergents, these molecules behave as unimolecular micelles capable of solubilizing hydrophobic molecules in aqueous solutions (Hawker et al., 1993).

Although a variety of new dendrimers has been synthesized in recent years, investigation of their physical and chemical properties has lagged (Hawker et al., 1995). In this work, we present vapor−liquid equilibrium data for binary solutions of dendrimers in a variety of organic solvents. This work supplements our earlier experimental studies on vapor−liquid equilibria for solutions of polyamidoamine (PAMAM) dendrimers (Mio et al., 1998).

Table 1. Solvent Properties

solvent	supplier	purity (%)
chloroform	Fisher Scientific	99.9
acetone	Fisher Scientific	99.7
triethylamine	Fisher Scientific	99
toluene	Fisher Scientific	99.9
tetrahydrofuran	Fisher Scientific	99+
acetonitrile	Fisher Scientific	99.9
n-hexane	Aldrich Chemical Co., Inc.	99+
n-heptane	Sigma-Aldrich	99+
n-octane	Aldrich Chemical Co., Inc.	99+
n-nonane	Aldrich Chemical Co., Inc.	99

Experimental Section

Materials. Solvents were degassed with a standard freeze−thaw procedure described by Panayiotou and Vera (1984) and used without further purification. Table 1 gives solvent properties.

Figure 1 shows dendrimers synthesized by surface modification of poly(propylene imine) dendrimers. Three series of dendrimers were studied with the same tertiary amine core structure but different surface groups. The A series and C series dendrimers are amber, viscous liquids at room temperature. They become darker and more viscous with rising generation number. The B series dendrimers are tan, semicrystalline solids at room temperature; their glass-transition temperatures were determined by differential scanning calorimetry and found to be near 85 °C. For subsequent calculations, all dendrimers are assumed to have a specific gravity of unity. Table 2 gives dendrimer properties.

Apparatus. Vapor−liquid equilibrium data were collected using a gravimetric-sorption method previously described by several authors (see, for example, Gupta and Prausnitz (1995)). Figure 2 shows a schematic diagram of the apparatus. The entire system is submerged in an isothermal water or air bath maintained at ±0.3 °C. A water bath was used for polymers with A surface groups; an air bath was used for polymers with B or C surface groups (see Figure 1).

---

* To whom correspondence should be addressed.

[†] Department of Chemical Engineering, University of California, Berkeley.

[‡] Department of Chemistry, University of California, Berkeley.

[§] Lawrence Berkeley National Laboratory.

10.1021/je980214k CCC: $18.00

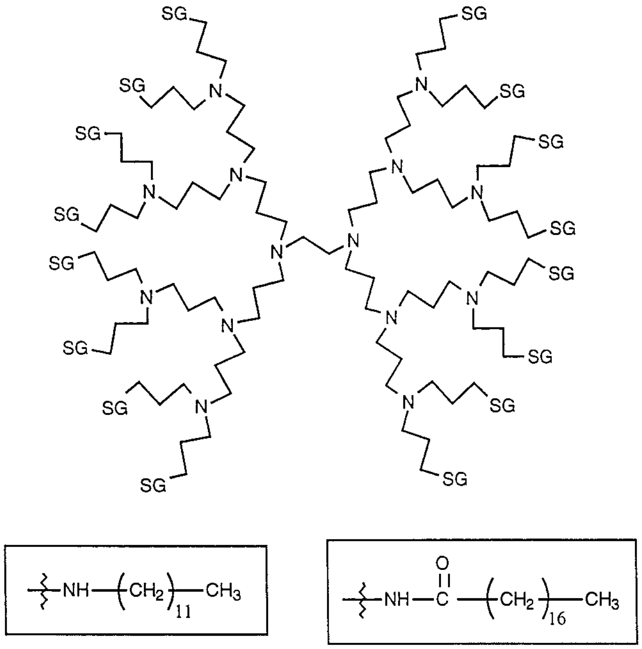

A-series surface group

B-series surface group

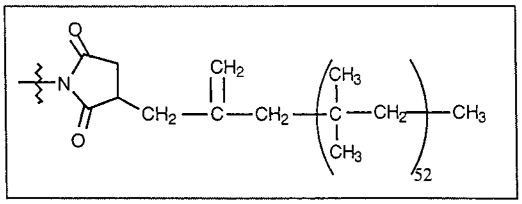

C-series surface group

Figure 1. Dendrimer structure (shown here is a generation three dendrimer with surface groups "SG").

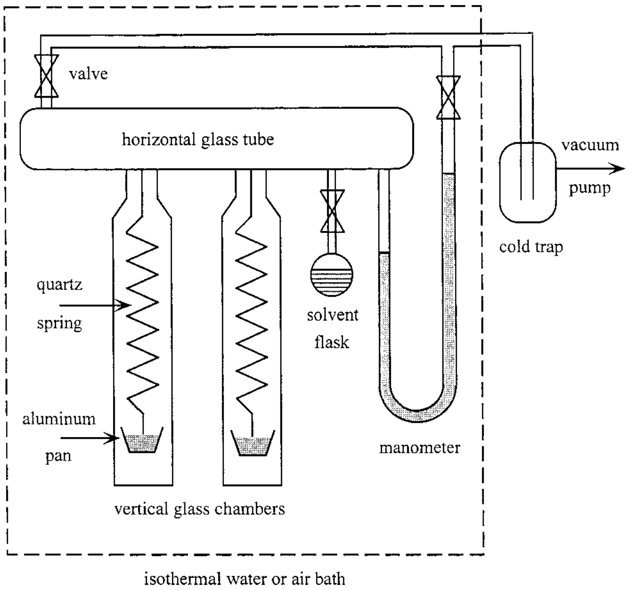

Figure 2. Experimental apparatus for vapor−liquid equilibrium measurements.

Each glass chamber contains one aluminum pan suspended from a quartz spring (Ruska Instruments Corp., Houston, TX). The calibrated springs have a sensitivity of about 1 mg/mm and a maximum load of 250 mg. Within this range, the elongation of each spring is linear with respect to change in mass.

A cathetometer (Wild, Heerbrugg, Switzerland) is used to measure the extension of the springs and the mercury levels of the manometer.

Experimental Procedure. Polymer samples of known mass (15−25 mg) are placed into previously weighed aluminum pans. The system is then vacuum-dried for 12−24 h to remove residual moisture and solvent. After obtaining the mass of dry polymer, solvent is introduced by opening and then closing the valve between the solvent flask and the evacuated glass chambers.

The system is allowed to equilibrate anywhere from 12 h to a few days after each solvent injection. Equilibrium is assumed when measurements in spring length do not change more than ±0.05 mm over a 12-h period.

Because the polymer is nonvolatile, the total pressure is equal to the vapor pressure of solvent above the polymer solution. Because experimental pressures are low (less than 1.1 bar), the solvent vapor is considered to be an ideal gas. Solvent activity a_1 is given by the ratio of the measured pressure to the pure solvent saturation pressure at system temperature.

The vernier scale on the cathetometer allows measurements to be made to the nearest 0.05 mm. Replicate measurements indicate that pressure and mass readings have a precision of 0.1 Torr and 0.1 mg, respectively. The uncertainty in solvent activity is 1−2% above $a_1 = 0.1$ and 2−4% below $a_1 = 0.1$. The solvent weight fraction w_1 uncertainty is 2−5% above $w_1 = 0.5$ and 5−10% below $w_1 = 0.5$.

The reliability of the apparatus and experimental procedure was established by reproducing published experimental vapor−liquid-equilibrium data for polystyrene in chloroform at 50 °C (Bawn and Wajid, 1956). The repro-

Table 2. Dendrimer Properties As Obtained from the Molecular Structures Shown in Figure 1

polymer[a]	mol wt of dendrimer	mol wt of surface groups	mol wt of core groups	no. of surface groups	no. of core groups[b]	surface group to core group ratio
A1	961	737	224	4	2	2.00
A2	2091	1474	617	8	6	1.33
A3	4351	2949	1402	16	14	1.14
A4	8870	5898	2972	32	30	1.07
A5	17911	11797	6114	64	62	1.03
B2	2876	2259	617	8	6	1.33
B3	5921	4519	1402	16	14	1.14
B4	12011	9039	2972	32	30	1.07
B5	24192	18078	6114	64	62	1.03
C1	12559	12335	224	4	2	2.00
C2	25287	24670	617	8	6	1.33
C3	50742	49340	1402	16	14	1.14
C4	101653	98681	2972	32	30	1.07

[a] The number after the letter represents the generation number. [b] Each tertiary amine group defines one core group.

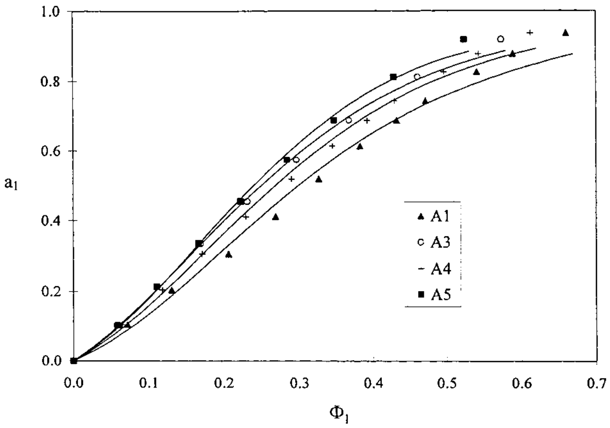

Figure 3. Calculated solvent activities (solid lines) for binary solutions of A series dendrimers in chloroform at 50 °C; data are poorly fitted with the theory by Hino et al.

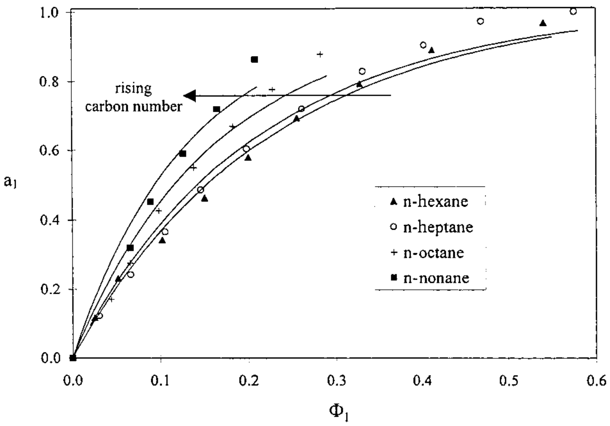

Figure 4. Calculated solvent activities (solid lines) for binary solutions of the A4 dendrimer in *n*-alkanes at 65 °C; data are poorly fitted with the modified lattice-cluster theory.

Table 3. Binary Systems Studied

polymer	solvent	*t* (°C)
A1, A3, A4, A5	chloroform	50
A1, A4	acetone	50
A2, A3, A5	triethylamine	65
A4	*n*-hexane	65
A4	*n*-heptane	65
A4	*n*-octane	65
A4	*n*-nonane	65
B2, B4, B5	*n*-heptane	75
B3, B4, B5	chloroform	70
B2, B4, B5	acetonitrile	75
C1, C3, C4	*n*-heptane	70
C1, C3	toluene	70
C2, C3, C4	tetrahydrofuran	50
C1, C3, C4	acetonitrile	70

ducibility in solvent activity was within ±5% of the previously published data.

Results and Discussion

Table 3 shows the binary systems studied, and Table 4 presents the vapor−liquid equilibrium data. Figures 3−12 show solvent activity a_1 as a function of solvent segment fraction Φ_1.

It is difficult to interpret the data with conventional polymer solution thermodynamics. At constant solvent activities, our results did not show higher solvent absorption for lower molecular weight dendrimers, contrary to expectations. Furthermore, the dependence of absorption on dendrimer generation number is sometimes not monotonic. For example, a dendrimer of generation five absorbs more than a dendrimer of generation four but less than a dendrimer of generation two. It appears that chemical interactions between solvent and dendrimer are significantly influenced by steric factors. At low generation numbers, we expect equal solvent access to dendrimer core groups and dendrimer surface groups; therefore, the composition of the entire dendrimer is important. However, at high generation numbers, surface group crowding may restrict solvent contact with core groups; therefore, the surface group composition may dominate solvent−

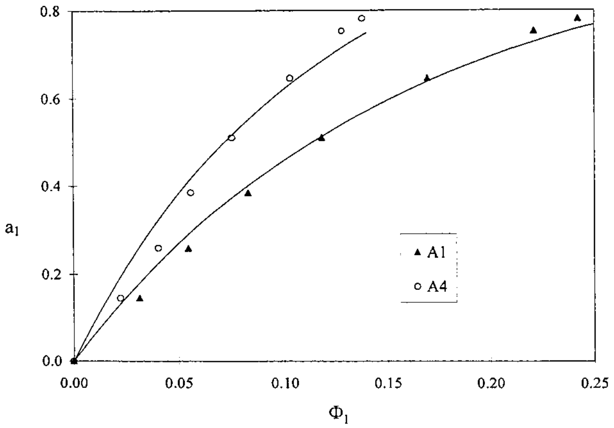

Figure 5. Calculated solvent activities (solid lines) for binary solutions of A series dendrimers in acetone at 50 °C; data are poorly fitted with the modified lattice-cluster theory.

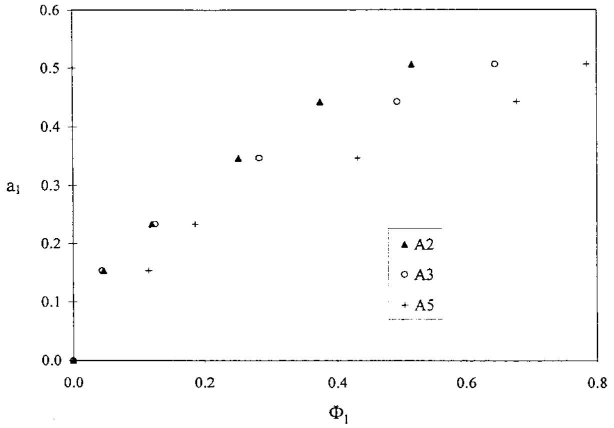

Figure 6. Solvent activity data for binary solutions of A series dendrimers in triethylamine at 65 °C.

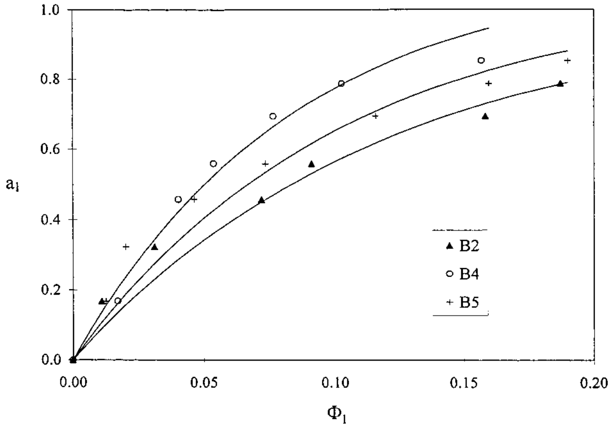

Figure 7. Calculated solvent activities (solid lines) for binary solutions of B series dendrimers in *n*-heptane at 75 °C; data are fitted with the modified lattice-cluster theory.

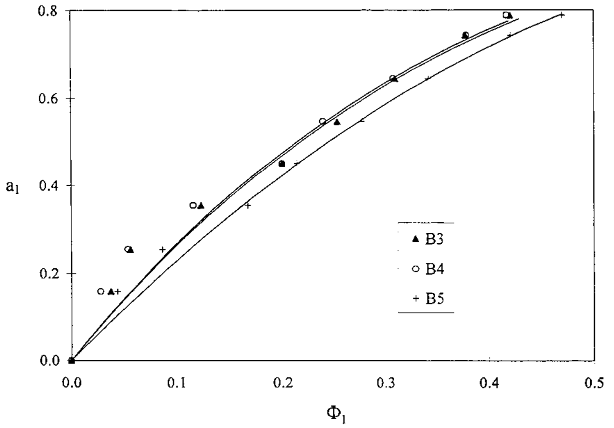

Figure 8. Calculated solvent activities (solid lines) for binary solutions of B series dendrimers in chloroform at 70 °C; data are fitted with the modified lattice-cluster theory.

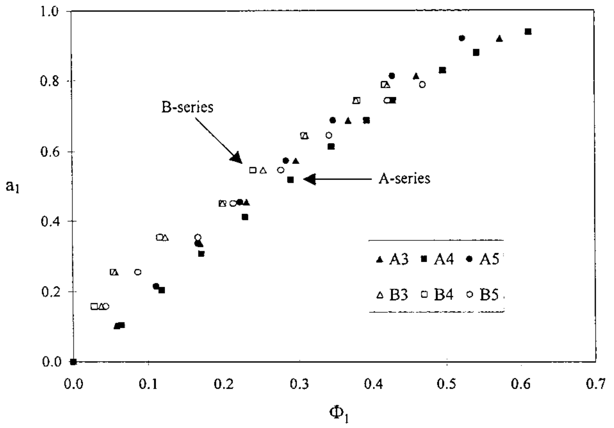

Figure 9. Comparison of solvent activities for the A series (50 °C) and the B series (70 °C) in chloroform.

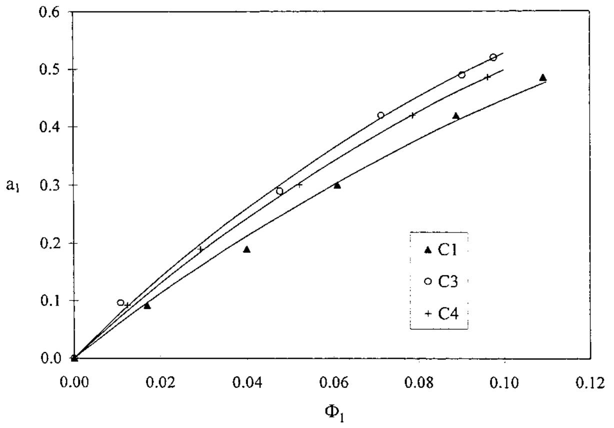

Figure 10. Calculated solvent activities (solid lines) for binary solutions of C-series dendrimers in *n*-heptane at 70 °C (the C series dendrimers are 99 wt % pure); data are fitted with the modified lattice-cluster theory.

dendrimer compatibility. For our dendrimers, the ratio of core groups to surface groups increases with rising generation number (Table 2), but the corresponding solvent accessibility to core groups probably decreases.

Steric hindrance provides a qualitative interpretation of our data. However, because these dendrimers are copolymers, intramolecular interactions between dissimilar copolymer segments may also be significant. For example, Gupta and Prausnitz (1996) showed that intramolecular repulsion in copolymers can strongly affect solvent absorption.

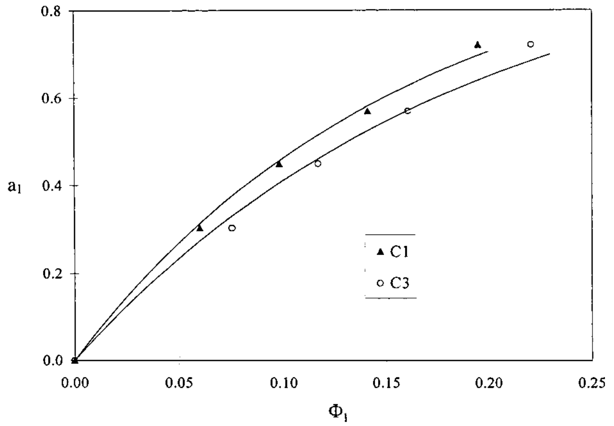

Figure 11. Calculated solvent activities (solid lines) for binary solutions of C series dendrimers in toluene at 70 °C (the C series dendrimers are 99 wt % pure); data are fitted with the modified lattice-cluster theory.

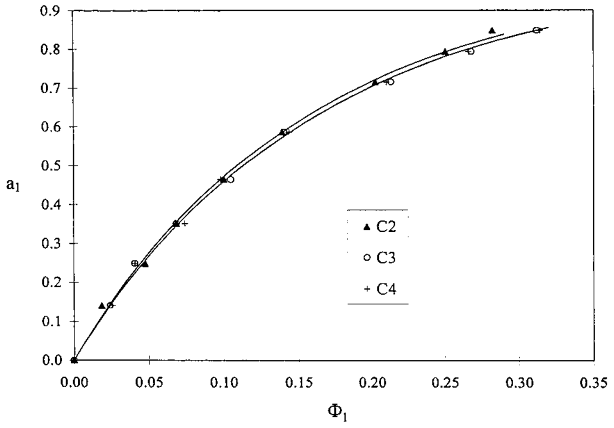

Figure 12. Calculated solvent activities (solid lines) for binary solutions of C″ series dendrimers in tetrahydrofuran at 50 °C (the C″ series dendrimers are 90 wt % pure); data are fitted with the modified lattice-cluster theory.

A Series Dendrimers. The A series dendrimers are terminated by dodecylamine surface groups. These dendrimers are expected to interact favorably with polar solvents due to amine surface groups and amine core groups, but only moderately with nonpolar solvents due to weak solvent interactions with dodecyl chains of the surface groups.

Figure 3 shows that A series dendrimers interact strongly with chloroform; the observed S-shaped absorption curves indicate hydrogen bonding between chloroform and dendrimers. The data show that A3 absorbs less chloroform than A1 and A4 dendrimers, perhaps because chloroform interactions with surface groups are more favorable than chloroform interactions with core groups. As the generation number rises, the surface group to core group ratio decreases, suggesting why A3 may absorb less than A1. With A4, surface group crowding may restrict solvent access to core groups; surface groups may therefore dominate interactions with the solvent, causing slightly increased solvent absorption relative to that in A3. The A5 dendrimer, however, absorbs the least chloroform, perhaps because steric hindrance restricts solvent−dendrimer contact.

Figure 4 shows results for solutions of A4 in C_6 though C_9 *n*-alkanes. Absorption decreases with rising alkane carbon number *n*. Alkane solvents have weak but favorable van der Waals interactions with dodecyl chains of the surface groups. These interactions are expected to become

Table 4. Vapor−Liquid Equilibrium Data

solvent = chloroform; t = 50 °C; P_1^{sat} = 526 kPa[c]

w_1(A1)[a]	w_1(A4)	a_1	w_1(A3)	w_1(A5)	a_1
0.100	0.090	0.105	0.081	0.083	0.103
0.178	0.162	0.205	0.154	0.152	0.215
0.272	0.229	0.307	0.227	0.223	0.336
0.345	0.299	0.412	0.301	0.291	0.455
0.410	0.369	0.519	0.377	0.362	0.574
0.471	0.430	0.614	0.455	0.433	0.688
0.522	0.481	0.688	0.551	0.518	0.812
0.562	0.519	0.744	0.659	0.612	0.918
0.628	0.586	0.827			
0.673	0.630	0.878			
0.736	0.694	0.937			

solvent = acetone; t = 50 °C; P_1^{sat} = 613 kPa

w_1(A1)	w_1(A4)	a_1
0.024	0.017	0.146
0.042	0.031	0.259
0.064	0.043	0.385
0.092	0.058	0.512
0.134	0.080	0.647
0.177	0.100	0.753
0.195	0.108	0.781

solvent = triethylamine; t = 65 °C; P_1^{sat} = 352 kPa

w_1(A2)	w_1(A3)	w_1(A5)	a_1
0.033	0.031	0.082	0.153
0.086	0.090	0.136	0.233
0.188	0.213	0.344	0.347
0.292	0.402	0.592	0.442
0.424	0.555	0.714	0.506

solvent = n-hexane; t = 65 °C; P_1^{sat} = 671 kPa

w_1(A4)	a_1	w_1(A4)	a_1
0.016	0.117	0.175	0.694
0.033	0.232	0.232	0.792
0.066	0.343	0.303	0.890
0.099	0.464	0.421	0.967
0.134	0.580		

solvent = n-heptane; t = 65 °C; P_1^{sat} = 255 kPa

w_1(A4)	a_1	w_1(A4)	a_1
0.020	0.122	0.186	0.720
0.044	0.243	0.243	0.829
0.071	0.367	0.304	0.904
0.100	0.487	0.364	0.972
0.138	0.604	0.467	1.000

solvent = n-octane; t = 65 °C; P_1^{sat} = 96 kPa

w_1(A4)	a_1	w_1(A4)	a_1
0.030	0.171	0.130	0.670
0.045	0.276	0.164	0.777
0.068	0.427	0.208	0.879
0.097	0.550		

solvent = n-nonane; t = 65 °C; P_1^{sat} = 37 kPa

w_1(A4)	a_1	w_1(A4)	a_1
0.046	0.320	0.119	0.720
0.063	0.453	0.152	0.863
0.090	0.591		

solvent = n-heptane; t = 75 °C; P_1^{sat} = 363 kPa

w_1(B2)	w_1(B4)	w_1(B5)	a_1
0.007	0.011	0.008	0.167
0.020		0.013	0.323
0.047	0.026	0.030	0.458
0.060	0.035	0.048	0.559
0.107	0.050	0.077	0.694
0.128	0.068	0.108	0.787
	0.106	0.130	0.853

solvent = chloroform; t = 70 °C; P_1^{sat} = 1022 kPa

w_1(B3)	w_1(B4)	w_1(B5)	a_1
0.052	0.039	0.060	0.159
0.077	0.074	0.117	0.255
0.164	0.155	0.219	0.354
0.258	0.258	0.275	0.451
0.321	0.305	0.348	0.547
0.385	0.383	0.420	0.645
0.459	0.460	0.504	0.743
0.504	0.500	0.553	0.788

solvent = toluene; t = 70 °C; P_1^{sat} = 204 kPa

w_1(C1)	w_1(C3)	a_1
0.050	0.063	0.304
0.082	0.098	0.449
0.119	0.136	0.570
0.166	0.189	0.722

solvent = n-heptane; t = 70 °C; P_1^{sat} = 305 kPa

w_1(C1)	w_1(C3)	w_1(C4)	a_1
0.011	0.007	0.008	0.092
0.026	0.031	0.019	0.190
0.040	0.047	0.034	0.301
0.059	0.060	0.052	0.419
0.073	0.065	0.064	0.485

solvent = tetrahydrofuran; t = 50 °C; P_1^{sat} = 439 kPa

w_1(C2)	w_1(C3)	w_1(C4)	a_1	w_1(C2)	w_1(C3)	w_1(C4)	a_1
0.016	0.021	0.022	0.141	0.121	0.122	0.125	0.587
0.041	0.035	0.035	0.248	0.178	0.188	0.185	0.715
0.059	0.059	0.064	0.351	0.222	0.238	0.236	0.793
0.087	0.091	0.085	0.465	0.251	0.279	0.281	0.848

[a] $w_1(Xi)$ = solvent weight fraction in the liquid phase with the X series dendrimer of generation i. [b] $a_1 = P/P_1^{sat}$ = solvent activity. [c] P_1^{sat} = pure solvent saturation pressure (calculated from equations suggested by Daubert and Danner (1989)) in kPa.

more favorable with rising n, as the alkanes become chemically similar to dodecyl chains. Solvent absorption decreases with rising n, however, perhaps due to steric factors; the A4 dendrimer has 32 surface groups in its outer shell, and larger solvent molecules may be hindered from penetrating the dendrimer molecule.

Figure 5 shows that absorption of acetone is low; the A1 dendrimer absorbs more acetone than the A4 dendrimer. A possible explanation is that acetone may interact more favorably with surface groups than with core groups. As generation number rises, the surface group to core group ratio decreases, suggesting why A4 may absorb less than A1.

Figure 6 shows absorption of triethylamine by the A series dendrimers. At 50% of the solvent vapor pressure, the solvent segment fraction exceeds 50%. Since structurally similar molecules often interact favorably, the similarity between triethylamine and tripropylamine core groups of the dendrimers may partially explain the unusually high solvent absorption.

B Series Dendrimers. Although our experimental temperatures were below glass-transition temperatures, the B series dendrimers liquefy upon solvent-induced melting, as indicated in Figures 7 and 8, where a significant increase in solvent absorption occurs at a solvent activity of about 0.4.

The dendrimers are terminated with octadecyl amide surface groups. Similar to those of the A series, these molecules are expected to interact favorably with polar solvents due to amide surface groups and amine core groups but only moderately with nonpolar solvents due to weak solvent interactions with the septadecyl chains of the surface groups.

Figure 7 shows that *n*-heptane is a moderate solvent for the B series. Absorption of *n*-heptane probably occurs through favorable van der Waals interactions between *n*-heptane and the septadecyl chains of the surface groups. The oxygen and nitrogen atoms of the amide surface groups and the amine core groups probably interact unfavorably with *n*-heptane. Raising the generation number from B2 to B4, there is a decrease in solvent absorption because of a decrease in the surface group to core group ratio. At B5, however, the increase in absorption may be due to surface group shielding of unfavorable solvent−core group interactions.

Figure 8 indicates high absorption of chloroform; B3 absorbs less than B5 and slightly more than B4. Similar to the case of the A series, interactions between chloroform and surface groups are probably more favorable than those with core groups. As the generation number rises, the surface group to core group ratio decreases, suggesting that B4 may absorb less than B3. With B5, however, increased solvent absorption may occur because dendrimer surface groups may dominate interactions with the solvent by crowding the dendrimer surface and limiting solvent access to dendrimer core groups.

Figure 9 shows that the A series dendrimers absorb more chloroform than the B series dendrimers, probably because B series dendrimers are near their glass-transition temperatures; molecular stiffness hinders solvent−dendrimer contact.

Acetonitrile is a very poor solvent for the B series dendrimers; it is not absorbed in significant quantities (not shown).

C Series Dendrimers. The C series dendrimers are terminated with polyisobutylene. These polymeric surface groups have the polydispersity approximately 1.5. Two sets of C series dendrimers were available, one with 99 and the other with 90 wt % purity. We refer to these as C and C″, respectively. Figures 10 and 11, respectively, show results for the C series dendrimers in *n*-heptane and toluene, and Figure 12 shows results for the C″ series dendrimers in tetrahydrofuran.

Figure 10 shows that C1 absorbs the most *n*-heptane, followed by C4 and then C3. *N*-Heptane probably interacts favorably with the long polymeric chains of the surface groups and unfavorably with the core groups. As the generation number rises, there is a decrease in the surface group to core group ratio, suggesting why C3 may absorb less than C1. With C4, surface group crowding may shield unfavorable solvent−core group interactions, thereby causing increased solvent absorption.

Figure 11 shows low absorption of toluene; C3 absorbs more than C1. Because toluene is an aromatic hydrocarbon, it may interact more favorably with amine core groups than with the nonpolar polymeric end chains of the surface groups, consistent with the absorption trend.

Figure 12 shows that absorption by C″ dendrimers exhibits no significant change with generation number, as expected, given the low purity of the C″ samples.

Acetonitrile is a very poor solvent for the C series dendrimers and not absorbed in significant quantities (not shown).

Attempts at Data Correlation. Liquid−liquid equilibrium data for some ordinary polymer solutions have been successfully correlated by a modified version of Freed's lattice-cluster theory by Hu et al. (1991a, 1991b). For hydrogen-bonded systems, a successful lattice model has been proposed by Hino et al. (1993). We therefore attempt to correlate our vapor−liquid equilibrium data with these theories.

Modified Lattice-Cluster Theory. Freed and co-workers (Bawendi and Freed, 1988; Freed and Bawendi, 1989) developed a lattice-cluster theory that avoids the mean-field approximation; it provides an improved description of the Flory−Huggins lattice. In Freed's theory, there are three contributions to the Helmholtz energy of mixing: the mean-field contribution plus two correction terms for energetic and entropic deviations from mean-field behavior. The Helmholtz energy of mixing ΔA is expressed by

$$\frac{\Delta A}{N_\mathrm{r}kt} = \left(\frac{\Phi_1}{r_1}\right)\ln\Phi_1 + \left(\frac{\Phi_2}{r_2}\right)\ln\Phi_2 + \sum_m\sum_n a_{mm}{\Phi_1}^m{\Phi_2}^n \qquad (1)$$

where N_r is the total number of lattice sites and k is the Boltzmann constant. Following Hu et al. (1991a), we revise Freed's theory by retaining only the first-order term of the entropic correction and multiplying it by a coefficient c_s. The solvent activity is then given by

$$\ln a_1 = \ln\Phi_1 + \left(1 - \frac{r_1}{r_2}\right)\Phi_2 + r_1[a_{11}{\Phi_2}^2 + a_{12}(-\Phi_1{\Phi_2}^2 + {\Phi_2}^3) + a_{21}(2\Phi_1{\Phi_2}^2) + a_{22}(-{\Phi_1}^2{\Phi_2}^2 + 2\Phi_1{\Phi_2}^3)] \qquad (2)$$

where

$$a_{11} = \frac{4}{9}c_\mathrm{s}\left(\frac{1}{r_1} - \frac{1}{r_2}\right)^2 + 2\tilde{e};\ a_{22} = -\frac{3}{2}c_2\tilde{e}^2;\ a_{21} = \frac{\tilde{e}}{r_2};\ a_{12} = \frac{\tilde{e}}{r_1}$$

As shown by Hu et al. (1991a), c_2 and c_s are found by fitting molecular simulation results for coexistence curves, giving 0.3 and 1.074, respectively. The solvent and polymer segment fractions, Φ_1 and Φ_2, are defined by

$$\Phi_2 = 1 - \Phi_1 = \frac{r_2N_2}{r_1N_1 + r_2N_2}$$

where N_1 and N_2 are the number of molecules and r_1 and r_2 are the number of segments per molecule of solvent and

Table 5. Parameters Used with the Modified Lattice-Cluster Theory

polymer	solvent	t (°C)	r_2	$\tilde{e}$ (interaction parameter)
A4	*n*-hexane	65	64	0.137
A4	*n*-heptane	65	57	0.164
A4	*n*-octane	65	52	0.235
A4	*n*-nonane	65	47	0.304
A1	acetone	50	13	0.276
A4	acetone	50	116	0.380
B2	*n*-heptane	75	18	0.356
B4	*n*-heptane	75	76	0.487
B5	*n*-heptane	75	154	0.400
B3	chloroform	70	69	−0.011
B4	chloroform	70	140	−0.008
B5	chloroform	70	283	−0.078
C1	*n*-heptane	70	80	0.227
C3	*n*-heptane	70	325	0.299
C4	*n*-heptane	70	651	0.273
C1	toluene	70	112	0.241
C3	toluene	70	453	0.183
C2	tetrahydrofuran	50	299	0.247
C3	tetrahydrofuran	50	600	0.234
C4	tetrahydrofuran	50	1203	0.234

polymer, respectively. We set r_1 equal to unity and calculate r_2 by

$$r_2 = \frac{M_2}{M_1}\frac{\rho_1}{\rho_2} = \frac{\text{molar volume of polymer}}{\text{molar volume of solvent}} \tag{3}$$

where M_1 and M_2 are the molecular weights and ρ_1 and ρ_2 are the mass densities of solvent and polymer, respectively. The dimensionless energy parameter $\tilde{e}$ characterizes the solvent−polymer interaction energy; the lower this parameter, the stronger the attraction between solvent and polymer. Table 5 gives values of $\tilde{e}$ and r_2.

Figures 10−12 show that the modified-lattice-cluster theory gives a reasonably good fit for C series dendrimers. Figures 4 and 5, however, indicate that the theory does not reproduce with the same accuracy VLE curves for A series dendrimers. Because B series dendrimers are semicrystalline at lower solvent activities, we only fit data above $a_1 = 0.4$, when it appears that the dendrimers have melted. Figure 8 shows that B series dendrimers in chloroform are reasonably fit for $a_1 > 0.4$. Figure 7 shows calculated curves for B series dendrimers in *n*-heptane for $a_1 > 0.4$. VLE data for the B2 and B5 dendrimers are fit reasonably, but data for the B4 dendrimer are fit poorly. Figure 6 shows solvent-activity data for the A series dendrimers in triethylamine; the data cannot be reasonably represented by the modified lattice-cluster theory.

Hydrogen-Bonded Systems. Solvent activity data for the A series dendrimers in chloroform exhibit S-shaped absorption patterns that are not reproduced by the modified lattice-cluster theory. Following Hino et al. (1993), we adopt an incompressible lattice model by ten Brinke and Karasz (1984) to introduce the effect of specific interactions into the Helmholtz energy of nonrandom mixing (Lambert et al., 1993). In Hino's theory, each contact point of a molecule is assumed to interact in a nonspecific manner with interaction energy ϵ_{ij} or in a specific manner with interaction energy $\epsilon_{ij} + \delta\epsilon_{ij}$, where $i = 1$ or 2 and $j = 1$ or 2. Assuming hydrogen bonding between solvent and polymer, the two necessary energy parameters are $\delta\epsilon_{12}$ and the interchange energy ϵ. Table 6 gives values for $\delta\epsilon_{12}$ and ϵ. Figure 3 shows calculated solvent activity curves for the A series dendrimers in chloroform.

Table 6. Parameters Used with Hino's Theory at 50 °C with Chloroform as Solvent

polymer	ϵ (J·mol^{-1})	$\delta\epsilon_{12}$ (J·mol^{-1})
A1	1.101	−5.351
A3	1.047	−5.356
A4	1.033	−5.306
A5	1.225	−5.453

Data for the B series dendrimers in chloroform do not show S-shaped absorption curves, perhaps because there is significant polymer crystallinity at the low solvent activities studied here.

Conclusions

Vapor−liquid equilibrium data for several binary dendrimer−solvent systems were obtained. The generation number and chemical composition of the dendrimer have a significant effect on solvent−dendrimer compatibility. On the basis of steric factors, a qualitative explanation was proposed to account for the dependence of solvent absorption on generation number.

Acknowledgment

The authors are grateful to Rebecca Brafman, Catherine W. Kuo, and Yonathan Thio, who assisted in data acquisition. The authors also thank John O. Tanbonliong and Cristina Mio for construction of the experimental apparatus and helpful comments.

Literature Cited

Bawendi, M. G.; Freed, K. F. Systematic Corrections to Flory−Huggins Theory: Polymer−Solvent−Void Systems and Binary Blend−Void Systems. *J. Chem. Phys.* **1988**, *88*, 2741−2756.

Bawn, C. E. H.; Wajid, M. A. High Polymer Solutions. Part 7. Vapour Pressure of Polystyrene Solutions in Acetone, Chloroform and Propyl Acetate. *Trans. Faraday Soc.* **1956**, *52*, 1658.

Daldrup, H. E.; Roberts, T. P. L.; Muhler, A.; Gossmann, A.; Roberts, H. C.; Wendland, M.; Rosenau, W.; Brasch, R. C. Macromolecular Contrast Media for MR Mammography. A New Approach to Characterizing Breast Tumors. *Radiologe* **1997**, *37*, 733−740.

Daubert, T. E.; Danner, R. P. *Physical and Thermodynamic Properties of Pure Chemicals*: *Data Compilation*; Hemisphere Publishing Corp.: New York, 1989.

Freed, K. F.; Bawendi, M. G. Lattice Theories of Polymeric Fluids. *J. Phys. Chem.* **1989**, *93*, 2194−2203.

Gao, H.; Carlson, J.; Stalcup, A. M.; Heineman, W. R. Separation of Aromatic Acids, DOPA, and Methyl-DOPA by Capillary Electrophoresis with Dendrimers as Buffer Additives. *J. Chromatogr. Science* **1998**, *36*, 146−154.

Gupta, R. B.; Prausnitz, J. M. Vapor-Liquid Equilibria for Copolymer/Solvent Systems: Effect of "Intramolecular Repulsion". *Fluid Phase Equilib.* **1996**, *117*, 77−83.

Gupta, R. B.; Prausnitz, J. M. Vapor−Liquid Equilibria of Copolymer + Solvent and Homopolymer + Solvent Binaries: New Experimental Data and Their Correlation. *J. Chem. Eng. Data* **1995**, *40*, 784−791.

Hawker, C. J.; Farrington, P. J.; Mackay, M. E.; Wooley, K. L.; Frechet, J. M. J. Molecular Ball Bearings: The Unusual Melt Viscosity Behavior of Dendritic Macromolecules. *J. Am. Chem. Soc.* **1995**, *117*, 4409−4410.

Hawker, C. J.; Wooley, K. L.; Frechet, J. M. J. Unimolecular Micelles and Globular Amphiphiles: Dendritic Macromolecules as Novel Recyclable Solubilization Agents. *J. Chem. Soc.*, *Perkin Trans. 1* 1993, *1*, 1287−1297.

Hino, T.; Lambert, S. M.; Soane, D. S.; Prausnitz, J. M. Lattice Thermodynamics for Binary Closed-Loop Equilibria: Ordinary and Polymer Systems. *AIChE J.* **1993**, *39*, 837−845.

Hu, Y.; Lambert, S. M.; Soane, D. S.; Prausnitz, J. M. Double-Lattice Model for Binary Polymer Solutions. *Macromolecules* **1991a**, *24*, 4356−4363.

Hu, Y.; Liu, H.; Soane, D. S.; Prausnitz, J. M. Binary Liquid−Liquid Equilibria from a Double-Lattice Model. *Fluid Phase Equilib.* **1991b**, *67*, 65−86.

Jansen, J. F. G. A.; de Brabander-van den Berg, E. M. M.; Meijer, E. W. Encapsulation of Guest Molecules into a Dendritic Box. *Science* **1994**, *266*, 1226−1229.

Jansen, J. F. G. A.; Meijer, E. W.; de Brabander-van den Berg, E. M. M. The Dendritic Box: Shape-Selective Liberation of Encapsulated Guests. *J. Am. Chem. Soc.* **1995**, *117*, 4417−4418.

Kukowska-Latallo, J. F.; Bielinska, A. U.; Johnson, J.; Spindler, R.; Tomalia, D. A.; Baker, J. R., Jr. Efficient Transfer of Genetic Material into Mammalian Cells Using Starburst Polyamidoamine Dendrimers. *Proc. Natl. Acad. Sci.* **1996**, *93*, 4897−4902.

Lambert, S. M.; Soane, D. S.; Prausnitz, J. M. Liquid−Liquid Equilibria in Binary Systems: Monte Carlo Simulations for Calculating the Effect of Nonrandom Mixing. *Fluid Phase Equilib.* **1993**, *83*, 59−68.

Mio, C.; Kiritsov, S.; Thio, Y.; Brafman, R.; Hawker, C. J.; Malmström, E. E.; Prausnitz, J. M. Vapor−Liquid Equilibria for Solutions of Dendritic Polymers. *J. Chem. Eng. Data* **1998**, *43*, 541−550.

Panayiotou, C.; Vera, J. H. Thermodynamics of Polymer−Polymer−Solvent and Block Copolymer−Solvent Systems. I. Experimental Measurements. *Polym. J.* **1984**, *16*, 89−102.

Shchepinov, M. S.; Udalova, I. A.; Bridgman, A. J.; Southern, E. M. Oligonucleotide Dendrimers: Synthesis and Use as Polylabeled DNA Probes. *Nucleic Acids Res.* **1997**, *25*, 4447−4454.

Singh, P.; Moll, F., III; Lin, S. H.; Ferzli, C.; Yu, K. S.; Koski, R. K.; Saul R. G.; Cronin, P. Starburst Dendrimers: Enhanced Performance and Flexibility for Immunoassays. *Clin. Chem.* **1994**, *40*, 1845−1849.

ten Brinke, G.; Karasz, F. E. Lower Critical Solution Temperature Behavior in Polymer Blends: Compressibility and Directional-Specific Interactions. *Macromolecules* **1984**, *17*, 815−820.

Wiener, E. C.; Konda, S.; Shadron, A.; Brechbiel, M. W.; Gansow, O. A. Targeting Dendrimer-Chelates to Tumors and Tumor Cells Expressing the High-Affinity Folate Receptor. *Invest. Radiol.* **1997**, *32*, 748−754.

Received for review August 28, 1998. Accepted March 4, 1999. This work was supported by the Director, Office of Energy Research, Office of Basic Energy Sciences, Chemical Sciences Division of the U.S. Department of Energy under Contract No. DE-AC03-76SF0098 and by the donors of the Petroleum Research Fund administered by the American Chemical Society.

JE980214K